Risk Assessment of Cable Discharge Events

Wolfgang Stadler, Josef Niemesheim, Andreas Stadler,
Sebastian Koch, Harald Gossner
Intel Deutschland GmbH, Am Campeon 10–12, D-85579 Neubiberg, Germany.
tel.: +49 (160) 89 35 308, e-mail: wolfgang.stadler@intel.com

Abstract – A rigorous measurement set-up, parameter extraction procedure, and SPICE simulation approach are presented which allows to assess the risk of ESD events caused by plugging a charged cable to a port of an electronic system (Cable Discharge Events). The feasibility of the approach is demonstrated on different USB-3 cables.

I. Introduction

During the last decade, Cable Discharge Events (CDE) have gained significant importance, especially in electronic systems communication interfaces like USB, Ethernet, Thunderbolt, Lightning, etc. Plugging in a charged cable or charged device (e.g., camera) into a port or vice-versa, plugging an uncharged cable into a port of a charged device will result in an electrostatic discharge (ESD). The severity of the ESD and the impact on the electronic system depends on many different factors, but most importantly the mechanical design of the connector (e.g., ground-first or shield-first contact) and the charge stored in the cable.

The first published works on CDE focus on the discharge waveform. The current waveform of a CDE can be described by a TLP-like square current pulse with an initial current spike [1-3]. The amplitude of the TLP plateau depends on the impedance of the CDE and the charging voltage, and the pulse width is a function of the length of the cable. The simple model of a transmission line is already sufficient to reproduce discharge waveforms of simple cables with well-defined boundary conditions. Examples are the discharge of the shield of a shielded cable into a ground or the discharge of a charged inner wire of a shielded cable with the shield grounded.

However, in real applications, the discharge of a cable shield or a ground wire into the ground of an electronic system might be considered as less critical. Although the fast transients might cause EMI disturbance and "soft errors," the risk of permanent damage (a "hard-failure") in the system is low. A direct discharge to a data line is considered to be much more severe. Due to the high bandwidth of state-of-the art communication interfaces the ESD protection measures are limited to ultra-low capacitance and low-insertion loss protection devices. The discharge of the inner wire of a shielded cable describes such a case if the shield is grounded first and then the data line contacts and discharges. However, it is often not known how much residual charge is stored on the data line before discharge, particularly in the case where the shield discharges to ground first. The charge stored on the inner wire determines the amplitude of the discharge current.

In recent work [4] a testing methodology for CDEs of Ethernet cables is discussed. The setup allows reproduction of real world scenarios of charging and discharging. Tamminen and Viheriaekoski [5] studied the current and voltage waveforms on the USB-2 data lines on a printed-circuit board (PCB).

The work presented here focuses on the modeling of the discharge via data lines. SPICE models are developed which reproduce the measured charging and discharging effects. The peak current and the width of the discharge pulse can be used for a rough estimation of required protection concepts. In a more comprehensive approach, SPICE models can be used for System Efficient ESD Design (SEED) approach using models of the PCB, protection elements, and the circuits including the discharge model of the cable.

The study is conducted on USB-3 cables, and, for comparison on a simple coax cable. In fact, most of the effects measured in an USB-3 cable can be explained with a coax cable model.

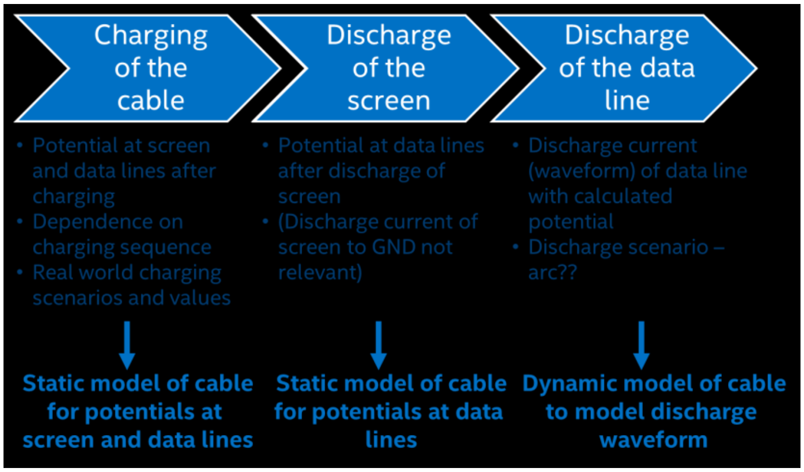

Figure 1: Steps to simulate the discharge wave form of a cable.

II. Measurement Techniques

A. Approach

For a simulation of the discharge, besides the discharge model of the cable itself, the charge (i.e., the voltage) stored on the data line before contact is the essential parameter. In this study, it turned out that the voltage on the data line before contact depends on the charging scenario and the discharge sequence of the cable, e.g., whether shield contacts first. Therefore, for the modeling of the discharge, three phases have to be evaluated (see Figure 1). In the case the shield contacts first, those steps are: First, the charging of the elements of the cable (shield, data lines …) prior to any contact to the port; secondly, the charging of the cable lines after the discharge of the shield, and third, the discharge of cable data line.

B. Experimental Set-ups

Figure 2 shows the overall view of the experimental set-up. The cable (here: USB-3 cable with C-type connector) is tied by several Nylon threads coming from the ceiling, in order to maintain a consistent height approximately 22 cm above the horizontal coupling plane (HCP) of a standard IEC table. The cable is connected to a USB-C port by a sliding mechanism (see Figure 3).

The USB-C port is shielded and the ground is connected to a vertical coupling plane (VCP). Each data line of the USB-C port can be connected to ground via a 2-ohm Pellegrini target (bandwidth 4 GHz). The sliding mechanism should guarantee a reasonable repeatability of the contact experiments.

On the far end of the cable, the wires of the cables are either cut and separated, or the cable is connected by an USB-C adaptor board to access all individual wires. Either the shield or each of the wires of the cable can be charged by a high-voltage source from 100 V to 5,000 V. Charging voltages up to approx. 2,500 V can be measured by a contact high-impedance digital voltmeter (TREK 821HH) with an input impedance of larger than 10^{14} Ω and an input capacitance of less than 10^{-14} F.

For the extraction of the capacitances of the cable shield to ground and the mutual capacitance between wires and between wires and shield, an Agilent B1500A Semiconductor Device Parameter Analyzer was used which enables measurements of capacitances with less than 1 pF. With a Prostat PRS-801 high-

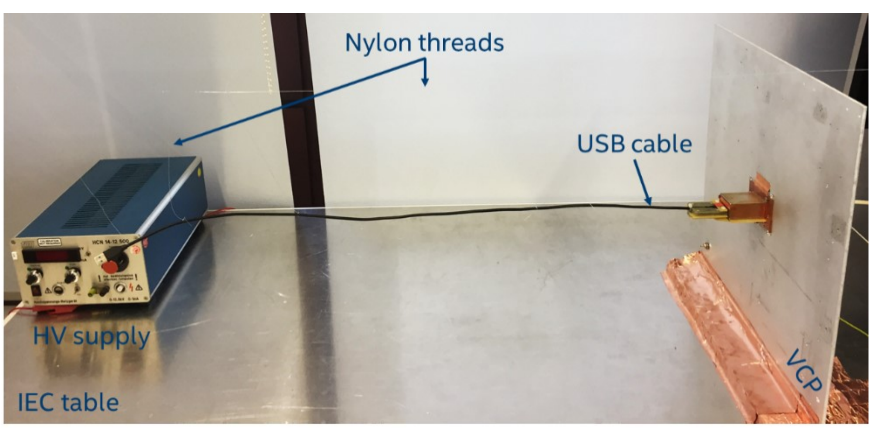

Figure 2: Overall view of the experimental set-up.

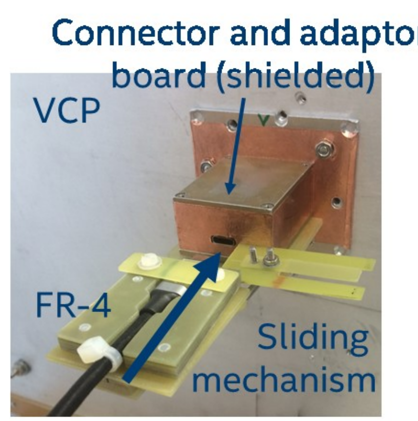

Figure 3: Sliding mechanism to connect the cable to the USB port

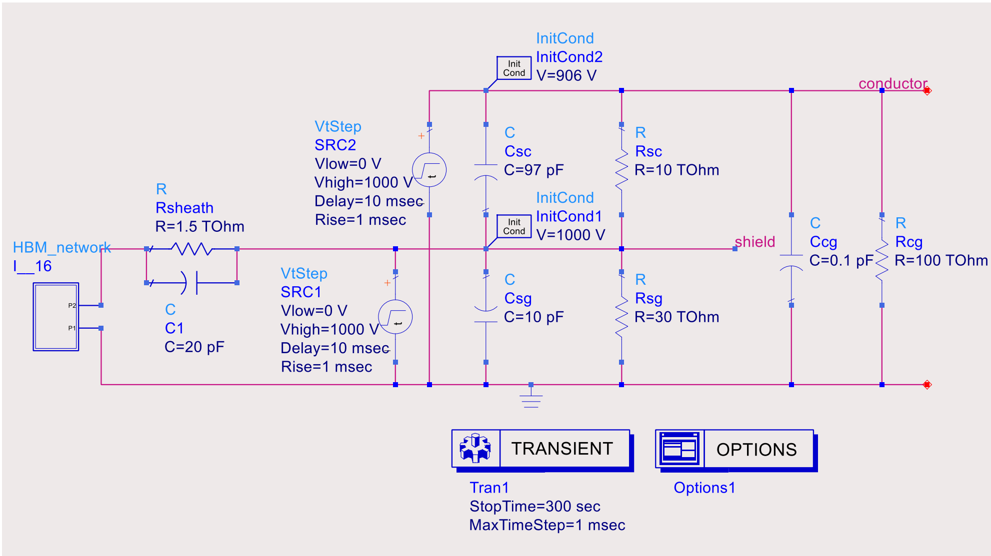

Figure 4: SPICE model used to simulate the charging process of a coax cable. Not all components are used for the different simulations.

resistance meter the resistances between wires and resistances of wires to shields are measured. Although the equipment allows measurements of rather low capacitances and rather high resistances, some of the parameters even exceed those measurement ranges and the corresponding parameters have to be estimated or deduced from indirect measurements.

III. Experimental Results and Modelling

A. Charging of the Cable

For the charging of the cable, static models including capacitances and resistances are in general sufficient as only a kind of steady-state a distinct period of time after the charging is of interest for the subsequent discharge. For a coaxial cable, the charging model is rather simple (Figure 4). It consists of resistances and capacitors between the shield and the conductor (R_{SC}, C_{SC}), between the shield and earth/ground, i.e., the HCP (R_{SG}, C_{SG}), and between the unshielded conductor pieces at the end of the cable to ground (R_{CG}, C_{CG}). The capacitance of the unshielded conductor is small compared to the other capacitance values and the resistance is much larger than the other resistance values. The capacitances of a 1 m long cable are measured as C_{SC} = 91 pF (data sheet: 97 pF), C_{SG} = 9.5 pF (theoretical calculation of wire above ground: 10 pF), and C_{CG} = 0.1 pF (theoretical calculation 0.04 pF). R_{SC} is given in the datasheet by ~10 TΩ. R_{SG} and R_{CG} cannot be measured nor calculated, but from the decay time of the charge (voltage) on the shield of ~300 s, R_{SG} can be estimated to ~30 TΩ.

Three different charging mechanisms are considered. In the first scenario, the shield is charged to high voltage (in Figure 5 and the following experiments: 1,000 V) and the conductor is floating. The initial voltage ratio between shield and conductor is given by the ratios of the capacitances C_{SC} and (C_{SC} + C_{CG}). In the model, we assume that the high voltage is applied to the shield for 60 seconds, resulting in a voltage at the conductor

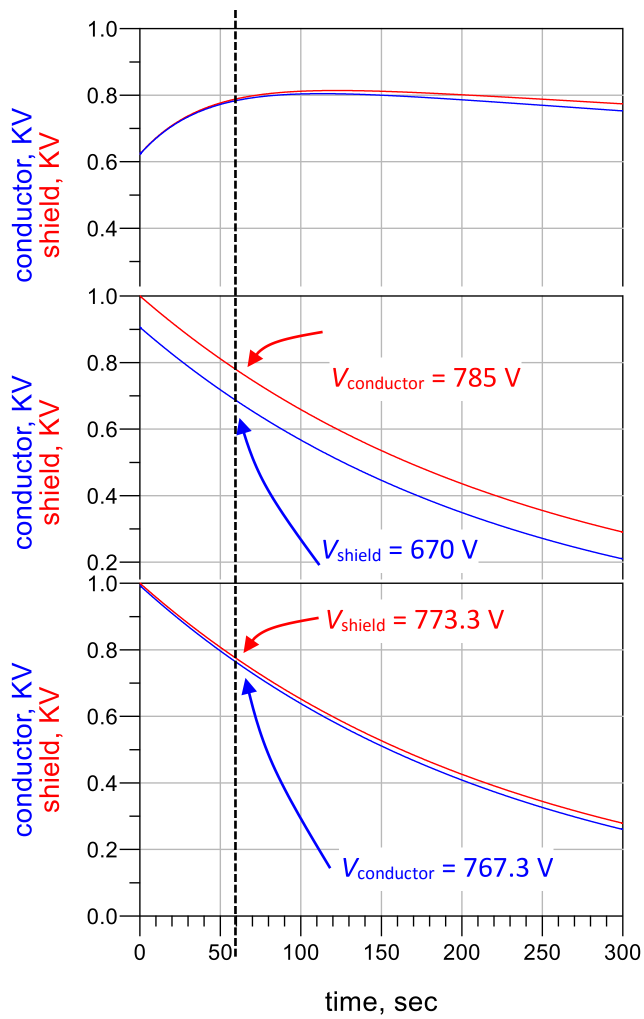

Figure 5: SPICE simulation of charging of the shield and the conductor of a coax cable; bottom: shield charged by HV; middle: conductor charged by HV; top: shield charged by a human being model

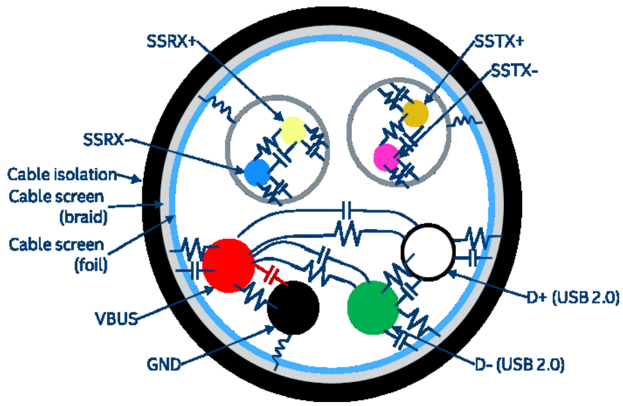

Figure 6: Cross section of an USB-3 cable with components used for the SPICE model.

of 999 V. Removing the HV source, the charging at the shield and at the conductor is decreasing simultaneously, but with slightly increasing voltage difference (after 300 s, the voltage difference between shield and conductor is ~6 V, see Figure 5, bottom). The simulated values agree very well with the measured values.

In the second scenario the conductor is charged while the shield is floating. The initial voltage at the shield determined by the ratio of C_{SC} and (C_{SC} + C_{SG}), hence the voltage difference between shield and conductor is significantly larger (~95 V) than in the first scenario. After one minute, the voltage difference increases to 105 V in this model (Figure 5, middle).

The third scenario models a human being touching the sheath of the cable. With standard HBM parameters (R_{HBM} = 1.5 kΩ, C_{HBM} = 100 pF) and a sheath resistance of 1.5 TΩ and a capacitive coupling C_{coupl} from the hand to the shield of 20 pF (see left part of the simulation model in Figure 4), the initial charging of the shield is mainly determined by the ratio of C_{coupl} and C_{sg}. The voltage difference between shield and conductor after 60 s is the same as in scenario #1.

An USB-3 cable is certainly much more complex. A typical cross section is shown in Figure 6. Obviously, the SPICE model is significantly more complex, too, a simplified model is drafted in Figure 7. Besides the parasitic circuit elements of the cable, there are also

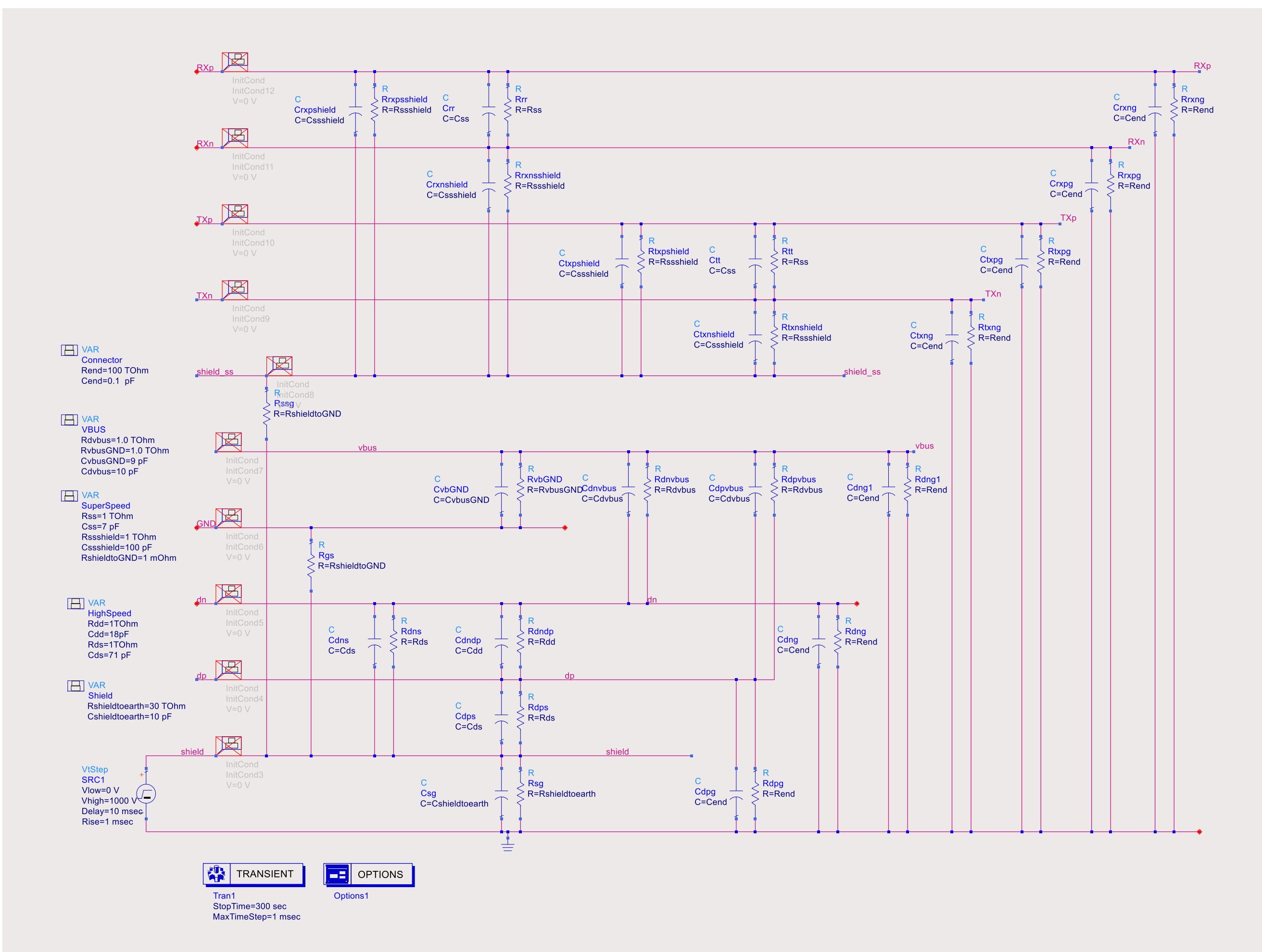

Figure 7: Simplified SPICE model used for charging of an USB-3 cable.

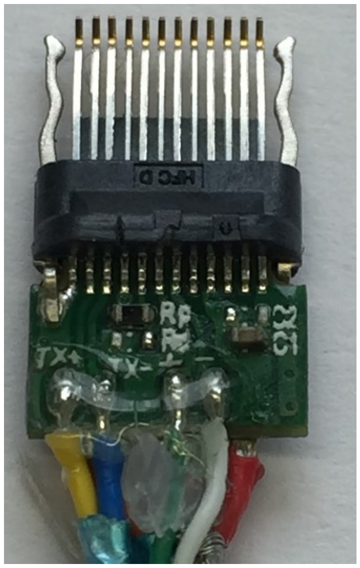

Figure 8: USB-3 connector with discrete resistors and capacitors

discrete elements in the connector (see Figure 8). However, the basic charging behavior is pretty much the same as in the simple coaxial cable. The voltage difference between shield and any data line or VBUS depends mainly on the charging scenario and the ratio of the capacitances. For one typical USB-3 cable, charging the shield results in a voltage difference of less than 5 V at all data lines; same for charging the cable by a human being. Charging ‘D+’ or any other data line leads to a roughly 100 V voltage difference between ‘D+’ and shield and a slightly higher voltage difference (~130 V) between ‘D+’ and the super-speed data lines. After removing the HV source, the voltage difference is decreasing, e.g., after 60 s the voltage at the shield is 500 V, at ‘D+’ 522 V, at ‘D-’ 512 V, and at ‘RX-’ 496 V. Hence, the most critical situation in terms of voltage difference is the immediate contact after removing the HV source.

It is important to note that USB-3 cables of different vendors are have different implementations. However, for most of the cables, the extracted capacitances and resistances are similar.

B. Discharging the Shield

In a next step, the simulated voltages on shield and the data and supply lines after charging with the three scenarios are taken as initial condition for the discharge of the shield to ground. The simulation models in Figures 4 and 7 are extended by a voltage dependent switch. As the discharge into the ground of a system is not in the focus of the study, a static model is sufficient. The outcome of the simulations and experiments are

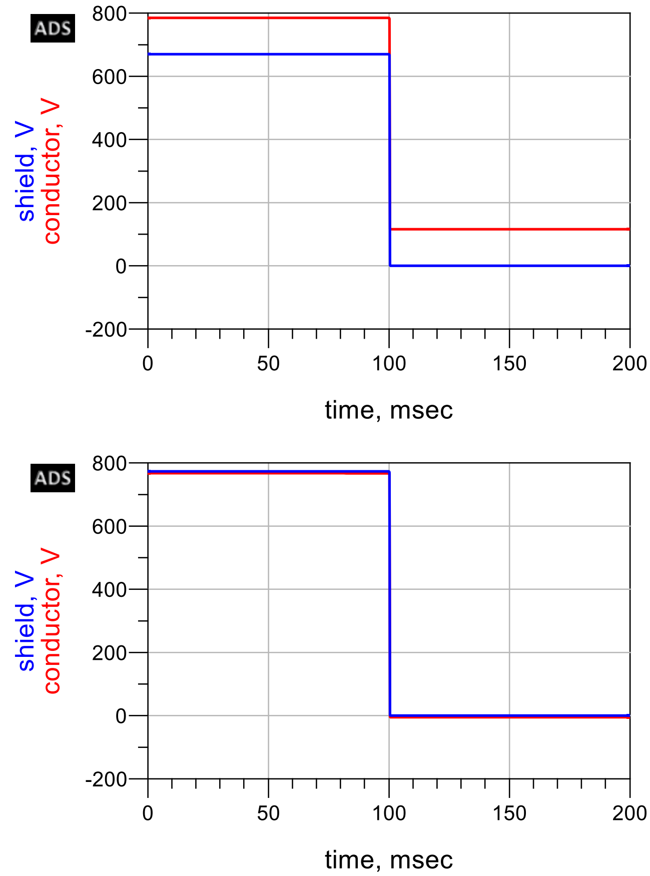

Figure 9: Discharge of the shield to ground of a coax cable; bottom: shield charged by HV; top: conductor charged by HV. The initial voltages are taken from Figure 4 after 60 s.

the voltages on the remaining conductors after shield contacts ground.

For both, coax cable and USB-3 cable, the charging of the conductors after shield contacts ground depend on the charging scenario. Figure 9 shows the voltages on the shield and the conductor of a coax cable. The initial voltages depend on the charging scenario, they are taken 60 seconds after the HV source was removed (see Figure 4). Charging the shield by a HV source or by a human being with floating conductor(s), after the ground conducts the shield (at t = 100 ms in Figure 9), the conductors have the negative potential of the initial potential difference. As the potential difference between shield and the conductors is small, i.e., in the coax cable of Figure 4 +6.0 V, the potential of the conductors is approx. -6.0 V after shield contacts ground.

The case that a data line is initially charged and then shield contacts ground is much more severe. The potential difference between conductor and shield remains constant. In the sample coax cable, the potential difference between conductor and shield is 105 V before the shield contacts ground (i.e., 50 s after

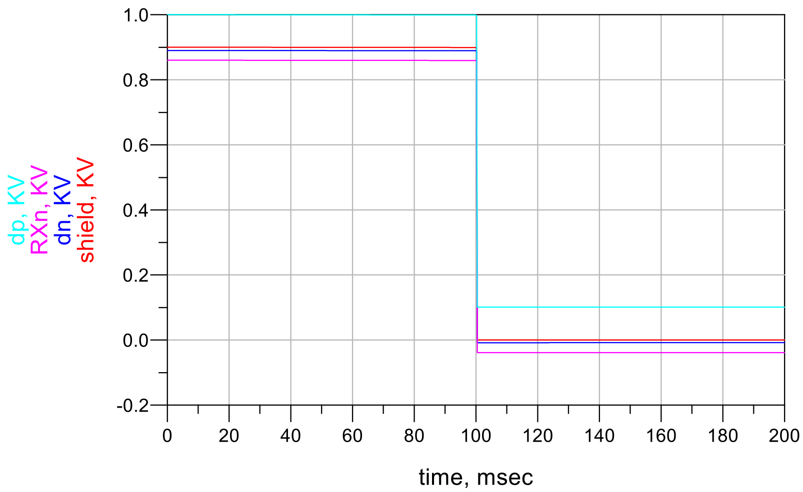

Figure 10: SPICE simulation of the potentials at some conductors of an USB-3 cable after grounding the shield at 100 ms. The cable was charged by a HV supply connected to D+

the HV source is removed) and again 106 V after the shield contacted ground. Obviously, the higher initial voltage difference results in a larger stored charge (larger voltage) on the conductor after the shield is grounded.

The third scenario in Figure 4 (human being touching the sheath of the cable) results in the same voltages on shield and conductor after 60 seconds. Hence the discharge scenario of the shield to ground can be described in the same way as in the first scenario (Figure 9, bottom).

It is not surprising that the discharge of the shield to ground of an USB-C cable is analog to the simpler coax cable. Again, if the shield is charged and 60 seconds later the shield contacts ground, the residual voltages on the data lines is in small, in the order of 5–7 V.

Figure 10 shows a simulation in which D+ of an USB-C cable is initially charged. After 100 ms, the shield is grounded. After grounding the shield, the initially charged 'D+' keeps the initial voltage difference to the shield, for this cable approx. 105 V. The potential difference of the other conductors – in Figure 9 'D-' (dn) and 'SSRX-' (RXn) – to shield remains constant after the shield is grounded (~20 V). All simulation results match the experimentally obtained data almost perfectly.

The potential at the conductors are used as initial conditions for the final simulation step.

C. Discharging the Conductor

From previous studies [1–3] it is well known that a cable discharge can be modeled by the discharge of a charged transmission line (TL). An ideal TL model as

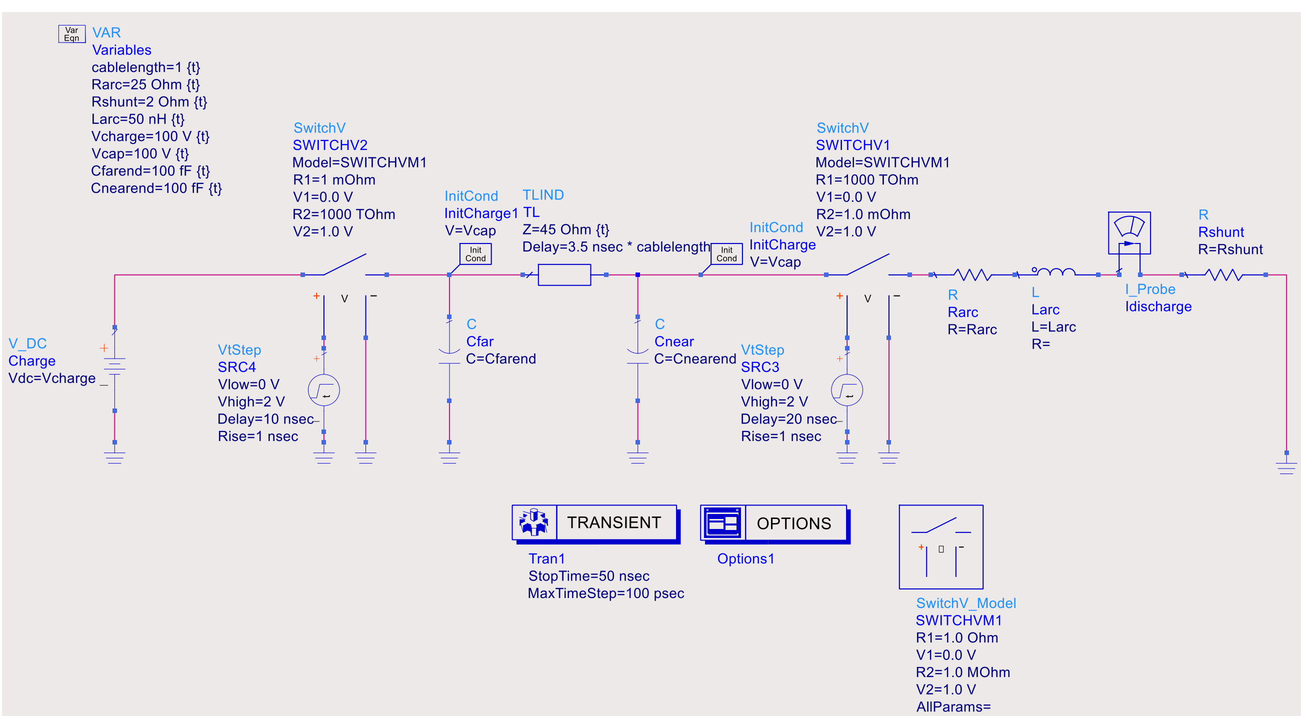

Figure 11: Example of a SPICE model used for the simulation of the discharge.

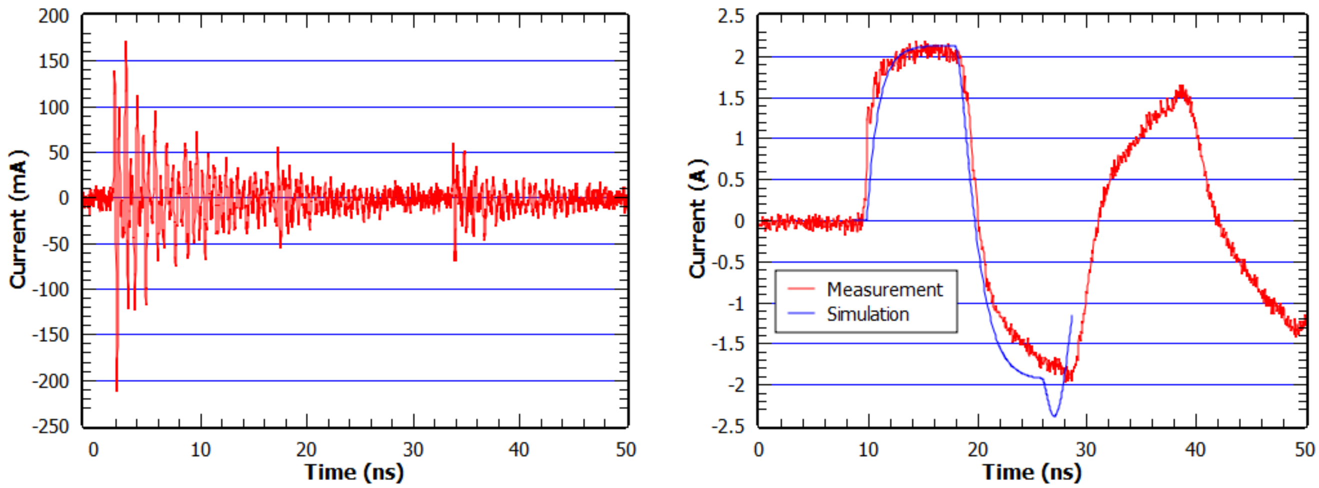

Figure 12: Measurement and simulation of an USB-3 cable, charged by a HV source at the D+ data line. Left: discharge of the shield (charged to ~900 V); right: measurement and simulation of the discharge of the D+ data line, following 1-2 ms after the discharge of the shield.

used for many SPICE simulators (Figure 11) has only two parameters, the impedance which is given by the cable type and the delay which is a function of the length of the cable and which can be calculated by 7 ns/m × l_{wire}. Capacitors at the far-end and the near-end of the TL account for capacitances of the connectors. Prior to the discharge, the TL is charged by a potential as determined by the DC simulation of the shield grounding. In addition to the 2-ohm shunt resistor of the Pellegrini target, a "static" (resistor R_{arc}, inductance L_{arc}) is included.

An example waveform of the many simulations and measurements of this study is shown in Figure 12. The D+ data line of an USB-3 cable (Type 1) is initially charged to 1,000 V. Then, the shield is discharged, and a discharge waveform (Figure 12, right) results from a coupling in the connector. The maximum discharge current is ~200 mA, the pulse widths of the coupling spikes are rather short, and hence, the energy transfer is low. The coupling depends on the exact design of plug and connector and the PCB connected to the connector.

Approximately 1–2 ms later, the data line D+ contacts the connector and discharges via a Pellegrini target to ground (Figure 12, right). Again, simulation agrees very well with the measured waveform.

Simulations and measurements behaves as expected. With a residual potential of ~100 V at the data line and an impedance of the data line D+ in an USB cable of 45 Ω, a "worst-case" discharge current of 2.2 A is calculated, with neglected arc resistance.

Simulations and measurements have been performed for the different charging scenarios and different cables. It was observed that the primary contributor to the severity of possible discharge currents are (1) charging mechanism, i.e., the charge on the data line which depends on this charging mechanism, and (2) the shield connection.

IV. Discussion

The results obtained by simulation and measurements can be assessed with respect to the severity of a discharge into an electronic component. Peak current and the energy of the pulse are the important design parameters for a "hard-failure" ESD protection concept with the SEED approach. For simple USB-3 cables, the maximum length is 3 m, resulting in a TL-like discharge with a pulse width of ~20 ns. A typical charging voltage of 1,000 V was selected which was in agreement with walking test in the office space at a relative humidity of 45% to 55%. Higher values could be possible in different environments or humidity. The peak currents vary significantly, depending on the charging scenario and the shield configuration:

1. A typical use case would be "charging the shield → discharging the shield during plug-in → discharging the data line". With the data lines of many commonly used USB-3 cable this seems to be less critical: for a charging voltage of 1,000 V the residual voltage at the data line is ~ 10 V, resulting in ~ 0.2 A.
2. The scenario "charging the data line (instead of shield) with screen floating → discharging the shield during plug-in → discharging the data line" is much more critical as typically the residual voltage at the data line is almost one order of magnitude larger: For a charging voltage of 1,000 V the residual voltage at the data line is

~100 V, resulting in ~2.5 A plateau current of the TL pulse for typical USB-3 cables.

3. During the study it turned out that not all USB cables have the shield connected to ground and/or not connected to the shell of the USB connector. In the worst case, the shield is not connected to ground and not connected to the USB connector shell at all. For the sequence as in scenario #1, "charging the shield → discharging the shield during plug-in (with no measured discharge current as the shield is not connected to the connector shell) → discharging the data line", the resulting discharge is the discharge of a TL with impedance to „earth") .For a charging voltage of 1,000 V and an impedance of $Z = 400\,\Omega$ (calculated by a theoretical impedance model of a wire to a metal plate), the current is similar to the scenario of the "good" cable and the data line charged, in our example ~2.2 A. However, the impedance to "earth" depends very much on the position of the cable and can be significantly lower, leading to much higher discharge currents, e.g., if the cable is lying on the ground.
4. The "worst worst case" is of course the situation that the shield is already grounded, and then the data line is charged to V_{charge} and immediate discharged. The resulting current at the data line is V_{charge} /(Z + R_{arc}) with V_{charge} = 1,000 V and Z = 45 Ω, the resulting discharge current exceeds 13 A. Practically, this situation can occur only if there is a discharge into the data line at the far-end of the cable. With an USB-3 compliant connector design, this is hardly possible; however, for special applications connectors exists which are not USB-3 compliant and have exposed data lines, power or ground (e.g., charger of sport watches, see photo in Figure 13).

Real-world examples of the different scenarios discussed above are listed in Table 1.

Figure 13: Charger of a sport watch with USB-2 connector. The data lines D+ and D- can be touched unintentionally. Scenario 4 describes the situation that the cable is first plugged in a PC, and then there is a discharge into D+ or D-.

The three-step approach demonstrated here can be easily transferred to any other cable, as. e.g., Ethernet, to assess the risk of a cable discharge event to any electronic component. Furthermore, more complex situations can be modeled without significant changes, for example the situation that an electronic device is connected to the far-end of the cable. In most cases the device is "only" an additional capacitance which will add the discharge of the capacitor at the end of the TL pulse (see [1]).

V. Conclusion

The charging and discharging scenarios of USB cables have been studied in detail and quantitative models are presented to accurately reproduce the observed discharge waveforms. This study allows to gain a deeper understanding of CDE stress conditions for the effective and efficient design of a protection circuit flowing the system efficient ESD design (SEED).

Table 1: Examples of real-world charging and discharging of the scenarios discussed in Section IV.

Test scenario	Example real world charging	Example real world discharging
1	Tribolectric charging of cable	Plugging of regular C-type USB cable
2	Charged device at far end without cable shield connected to device	Plugging of regular C-type USB cable
3	Tribolectric charging of cable	Plugging of regular C-type USB cable without first mate ground contact of cable shield
4	Charged device at far end without cable shield connected to device	C-type USB cable plugged into victim device with shield connected to ground of victim device

To cover most stress events of USB cables with a length between 1 m and 3 m, a stress level of a few Amperes for up to roughly 20 nanoseconds duration should be assumed for the protection design (SEED).

For use cases where high quality, fully compliant USB cables and connectors can be expected like for server applications, the CDE stress current level is in the regime of several 100 mA up to 2 A, depending on the charging level, with a stress duration of ~20 nano-seconds.

The extreme condition of a non-compliant cable or connector in combination with a charged device discharging into a data line leading to discharge current beyond 10 A is in general non practical to protect on IC and PCB level for typical high performance consumer systems. This requires better control of cable and connector design and manufacturing.

Acknowledgements

The authors would like to acknowledge the ESD Association mentor Jeff Dunnihoo (Pragma Design) and Prof. David Pommerenke (Missouri University of Science and Technology, Rolla, MO) and his team for their valuable comments and feedback. We thank Intel's ESD experts Brett Carn, Nathan Jack, Ben Orr, Franz Zaengl, and Peyman Ensaf for their continuous great support and the many fruitful discussions.

References

[1] W. Stadler, T. Brodbeck, R. Gärtner, H. Gossner, "Cable Discharges into Communication Interfaces", EOS/ESD Symposium 2006, 144.

[2] S. Poon, T. Maloney, "Shielded Cable Discharge Induces Current on Interior Signal Lines", EOS/ESD Symposium 2007, 311.

[3] W. Stadler, T. Brodbeck, J. Niemesheim, R. Gaertner, K. Muhonen "Cable Discharges into Communication Interfaces", EOS/ESD Symposium 2009, 419.

[4] W. Huang, J. Tichenor, D. Pommerenke, V. Pilla, P. Maheshwari, G. Maghlakelidze, "An Ethernet Cable Discharge Event (CDE) Test and Measurement System", EMC 2014, 301.

[5] P. Tamminen, T. Viheriäkoski, "Charged Cable–System ESD Event", EOS/ESD Symposium 2016.